Delocalized Wigner lattice on a dielectric layer with a metallic substrate: Dynamical properties and phase transitions

Lenac, Z.; Šunjić, Marijan

Delocalized Wigner lattice on a dielectric layer with a metallic substrate: Dynamical properties and phase transitions

Z. Lenac

Pedagogical Faculty, 51000 Rijeka, Croatia

M. Šunjić

Department of Physics, University of Zagreb, P.O.B. 162, 41000 Zagreb, Croatia

Properties of a two-dimensional Wigner lattice are analyzed taking into account delocalization of electrons on a thin dielectric layer with a metallic substrate. Electronic screening arising from the metallic substrate enhances the image potential as compared to the semi-infinite dielectric layer, but at the same time lowers the electron-electron interaction. As a result, the electron delocalization becomes a complicated function of the dielectric thickness, dielectric constant, and the electron density. The electron ground-state energy is calculated including the $k = 0$ term of the lattice potential, which has a significant effect at high electron densities. The influence of electron delocalization and of the dielectric substrate on the electron lattice dynamics (phonon spectra, sound velocities) and on the Wigner phase transition is demonstrated. In particular, possible extension of the Kosterlitz-Thouless melting criterion to the quantum regime is discussed.

I. INTRODUCTION

The existence of a two-dimensional (2D) Wigner lattice on a dielectric substrate has been confirmed experimentally more than ten years ago.[1] The main problem preventing more detailed experimental studies of this lattice is the weakness of the image potential which traps electrons above the dielectric surface only for low electron concentrations. A metallic substrate[2,3] or a dielectric with high dielectric constant[4,5] placed below a thin dielectric layer (usually liquid helium) can significantly enhance the attractive image interaction, eventually leading to the formation of a Wigner lattice at higher electron densities. However, strong image force can also cause tunneling of electrons through the thin dielectric into the metal substrate. The calculations performed for He (Ref. 6) show that the He thickness should be > 35 Å to prevent appreciable tunneling effects. In that case, an upper limit of electron concentration is estimated to be $\approx 2 \times 10^{12}$ cm^{-2}.

In our previous papers,[7,8] here denoted by I and II, respectively, we have studied the Wigner lattice on a semi-infinite dielectric substrate by taking into account (i) finite electron size (delocalization) and (ii) the dielectric properties of the substrate. The presence of a metallic substrate changes the dielectric response of the system, and the electron-electron interaction is strongly modified due to additional screening. But it could also change dramatically the electron delocalization, so here we want to discuss the influence of such an effect on the dynamical properties of the Wigner lattice, and particularly on the criteria for the Wigner phase transition.

In the classical model, where electrons are described as point particles localized at a distance d above the metallic substrate,[2-4] the influence of this substrate is described

by a single parameter d / ρ, where ρ is the (average) distance among the two electrons. In our approach, we start at the density and temperature where the electrons form a Wigner lattice on a dielectric layer of thickness d deposited on a metallic substrate. The lattice oscillates in the ρ direction (parallel to the dielectric surface) and has a finite delocalization Δz in the (perpendicular) z direction. As a consequence, the properties of the system are determined by three parameters: ρ, d, and Δz, and the "scaling" with d / ρ is no longer valid. However, for given ρ and d, the third parameter Δz can be determined by minimizing the total energy of the Wigner lattice.[7,8]

The paper is organized as follows. In Sec. II we discuss the influence of the metallic substrate on electron-electron interaction for various ratios of the three characteristic length parameters ρ, d, and Δz. In Sec. III we analyze the dynamical properties of the system, and in Sec. IV we calculate the Wigner phase transition diagrams, primarily their dependence on the dielectric thickness. The conclusions are given in Sec. V.

II. ELECTRON-ELECTRON INTERACTION: INFLUENCE OF A METALLIC SUBSTRATE

The model Hamiltonian of electrons in a Wigner lattice on a dielectric layer of thickness d deposited on a (semi-infinite) metallic substrate has a form[8]

$$H = \sum_i K_i + \sum_i W^{im}(z_i) + \frac{1}{2} \sum_{j \neq i} W^{ee}(\rho_{ij}; z_i, z_j) . \quad (1)$$

The first term is the electron kinetic energy, the second is the image potential felt by the electron i at the distance z_i above the dielectric surface, and the third term describes the total interaction (including images) between all the

electrons (i,j), at a lateral distance $\rho_{ij}=|\boldsymbol{\rho}_i-\boldsymbol{\rho}_j|$ (lattice potential).

A. Image potential

We describe the metallic substrate as an ideal metal that instantaneously and completely screens the electron charge e. Therefore, the image potential of an electron at a distance z above the dielectric surface is given in the two-dimensional Fourier $\mathbf{k}$ space as[7,8]

$$W^{\mathrm{im}}(z)=-\tfrac{1}{2}e^2\int d\mathbf{k}\,D(k)e^{-2kz}\,,\qquad(2)$$

and the "response" function $D(k)$ is[9]

$$D(k)=\frac{\beta+e^{-2kd}}{1+\beta e^{-2kd}}\,.\qquad(3)$$

In the $d\to\infty$ limit we find the standard result for the semi-infinite dielectric substrate, with the dielectric constant ϵ:

$$D(k)\xrightarrow[d\to\infty]{}\beta\equiv\frac{\epsilon-1}{\epsilon+1}\,.\qquad(4)$$

In order to study the effects of the metallic substrate on the image potential, we can expand $D(k)$ in powers of β $(\beta<1)$:

$$D(k)=\sum_{n=-1}^{\infty}b_n e^{-2(n+1)kd}\,,$$
$$b_{-1}=\beta,\quad b_n=(-1)^n(1-\beta^2)\beta^n\,.\qquad(5)$$

The condition for perfect screening (or charge neutrality) due to the presence of a metallic substrate is obtained from the sum rule:

$$D(0)=\sum_{n=-1}^{\infty}b_n=1\,.\qquad(6)$$

It holds for finite d and in the limit $d\to\infty$ (the metallic substrate is infinitely far from the lattice). The $d=\infty$ limit [no metallic substrate: $D(0)=\beta<1$] is physically different. In the former case, the metallic substrate provides the charge neutrality, while in the latter case it should be done by an external field.[3,10]

With the help of Eq. (5), the image potential (2) can be easily integrated to give an infinite series of electron images:[11]

$$W^{\mathrm{im}}(z)=-\frac{e^2}{4}\sum_{n=-1}^{\infty}\frac{b_n}{[z+(n+1)d]}\,.\qquad(7)$$

Usually the parameter β is small $(\beta\lesssim0.3)$ so one can keep only the linear terms in β:

$$W^{\mathrm{im}}(z)=-\frac{e^2}{4}\left[\frac{1}{(z+d)}+\beta\left[\frac{1}{z}-\frac{1}{z+2d}\right]+O(\beta^2)\right]\,.\qquad(8)$$

Notice that in some limiting cases $W^{\mathrm{im}}(z)$ takes a simple form

$$W^{\mathrm{im}}(z)\to-\tfrac{1}{4}(e^*)^2\frac{1}{z}\,,$$
$$e^*=\begin{cases}e,&d\to0\text{ or }z\to\infty\\e\sqrt{\beta},&d\to\infty\text{ or }z\to0\,.\end{cases}\qquad(9)$$

Therefore, we expect that the ground-state wave function appropriate for the $1/z$ potential,[12,13]

$$u(z)=2\alpha^{3/2}ze^{-\alpha z}\qquad(10)$$

will be an excellent approximation for the "perpendicular" Schrödinger equation, which contains the image potential (2). From I and II we expect that (10) will also be a good "perpendicular" trial wave function for the minimization of the full Hamiltonian (1). Thus determined parameter α gives the electron perpendicular width Δz and the mean perpendicular position $\langle z\rangle$ of the electron:

$$\Delta z=\sqrt{3}/2\alpha,\quad\langle z\rangle=3/2\alpha\,.\qquad(11)$$

The image energy of an electron evaluated with the wave function (10) is

$$\langle E^{\mathrm{im}}\rangle\equiv\langle K(z)\rangle+\langle W^{\mathrm{im}}(z)\rangle$$
$$=\frac{e^2}{2}a_0\alpha^2-\frac{e^2}{2}\int_0^\infty dk\frac{D(k)}{(1+k/\alpha)^3}\,,\qquad(12)$$

where a_0 is the Bohr radius.

B. Lattice potential

Following Refs. 7 and 8 we can derive the influence of the metallic substrate on the lattice potential in 2D $\mathbf{k}$ space: we have to insert the full expression (3) for $D(k)$ instead of the parameter β in the term that describes the electron-image interaction in Eq. (6) in Ref. 7. After integration, we obtain the z-averaged lateral interaction between the two electrons:

$$\langle W^{ee}(\rho)\rangle=\int\int|u(z)|^2 W^{ee}(\rho;z,z')|u(z')|^2dz\,dz'$$
$$=\frac{e^2}{\rho}\int_0^\infty dx\,J_0(x)\frac{1}{(1+ax)^3}$$
$$\times\left[1+\tfrac{3}{8}ax(3+ax)-\frac{D(x/\rho)}{(1+x)^3}\right]\,.\qquad(13)$$

where J_0 is the Bessel function and $a=1/2\alpha\rho$.

In discussing the limiting cases, we have to compare three length parameters α^{-1}, ρ, and d, while in the point-electron $(\alpha\to\infty)$ approximation, $\langle W^{ee}\rangle$ is the function of one parameter $\langle\rho/d\rangle$ only.[3]

(i) Low-density limit: $\rho\gg\alpha^{-1}$, i.e., $a\ll1$. The electrons are well separated $(\rho\gtrsim300\text{ Å})$, and the influence of the image potential due to the presence of the metallic substrate is relatively strong. For a very thick dielectric $(d\gg\rho)$ the monopole interaction dominates:

$$\langle W^{ee}(\rho)\rangle\to\left[(1-\beta)-\tfrac{1}{2}(1-\beta^2)\frac{\ln(1+\beta)}{\beta}\right]\left[\frac{\rho}{d}\right]$$
$$-3(1-7\beta)\frac{1}{(2\alpha\rho)^2}\right]\frac{e^2}{\rho}\,,\qquad(14)$$

but for a thin dielectric film $(d \ll \rho)$ the interaction takes the dipolar form:

$$\langle W^{ee}(\rho) \rangle \rightarrow \frac{1}{\alpha^2} \left[\frac{9}{2} + 6 \left[\frac{1-\beta}{1+\beta} \right] (\alpha d) \right.$$

$$\left. + 2 \left[\frac{1-\beta}{1+\beta} \right]^2 (\alpha d)^2 \right] \frac{e^2}{\rho^3} . \qquad (15)$$

In the last expression the role of finite α is particularly important.

(ii) High-density limit: $\rho \ll \alpha^{-1}$, i.e., $a \gg 1$. The electrons are laterally very close in comparison with their average distance from the substrate $\langle z \rangle = 1.5\alpha^{-1}$, so the influence of the substrate is negligible. The lateral interaction exhibits a characteristic logarithmic behavior:

$$\langle W^{ee}(\rho) \rangle \rightarrow e^2 2\alpha [\tfrac{3}{8} \ln(1/2\alpha\rho) + \tfrac{1}{2} + O(2\alpha\rho)] . \qquad (16)$$

For a typical value $\alpha^{-1} \sim 40 a_0$, the high-density limit is achieved for $\rho \lesssim 10$ Å. However, such high densities cannot be obtained experimentally.[6]

The total lattice potential in the Hartree approximation is obtained as a lattice sum of $\langle W^{ee}(\rho) \rangle$:

$$\langle W^{ee} \rangle = \sum_{l \neq 0} \langle W^{ee}(\rho_l) \rangle . \qquad (17)$$

Here ρ_l are the regular electron lattice sites. As shown in I, we can neglect the lateral spread of the electron wave function (σ) and take only the z average of $W^{ee}(\rho)$ (17) in order to determine the "delocalization parameter" α. In II we have thus derived the dynamical properties of a delocalized lattice. A similar approach shall now be applied to the Wigner lattice on a finite dielectric layer with a metallic substrate.

III. DYNAMICAL PROPERTIES OF A WIGNER LATTICE

Although electron-electron interaction has a simple form (13) in **k** space, this form is not convenient for evaluating the lattice sum (17). The procedure of deriving the ground-state energy and the eigenfrequencies of the lattice was discussed in detail in Appendixes of I and II, respectively. In the Appendix of this paper we show how we can include the influence of a metallic substrate into these considerations by simply redefining the function $f(x)$ which enters into the definition of the electron-electron interaction in "x".[7,8]

A. Average electron-electron interaction

At this point we draw particular attention to the average electron-electron interaction, defined as

$$\langle W_0^{ee} \rangle = \frac{1}{S} \int d\rho \langle W^{ee}(\rho) \rangle , \qquad (18)$$

where S is the average area per electron. In **k** space we find [Eq. (7), Ref. 7]

$$\langle W_0^{ee} \rangle = \int dz |u(z)|^2 \int dz' |u(z')|^2 w(k \rightarrow 0; z, z') ,$$

$$w(k \rightarrow 0; z, z') = \frac{2\pi}{S} e^2 \lim_{k \to 0} \left[[1 - D(k)] \frac{1}{k} + D(k)(z + z') \right.$$

$$\left. + |z - z'| \right] . \qquad (19)$$

In the case of a semi-infinite dielectric $(d = \infty)$, with $D(k) = \beta$, $\langle W_0^{ee} \rangle$ obviously diverges for $\beta < 1$ because of the lack of charge neutrality in the system. For the same reason, the lattice potential $\langle W^{ee} \rangle$ also diverges. To prevent this divergency, the system is assumed to be embedded in a uniform background of positive charge.[10] This additional interaction in fact cancels the $\langle W_0^{ee} \rangle$ term, so it should be substracted from the lattice ground-state energy, which makes that energy finite.[7]

The situation becomes quite different in the case of a dielectric layer on a metallic substrate. Using Eq. (5) for $D(k)$, we find from (19) and (10)

$$\langle W_0^{ee} \rangle = \frac{2\pi}{S} e^2 \left[\left[\frac{1-\beta}{1+\beta} \right] 2d + \frac{33}{16} \frac{1}{\alpha} \right] , \qquad (20)$$

which remains finite for finite d because of the perfect electron screening in the presence of a metallic substrate. In the Appendix we have shown that the lattice potential and therefore the ground-state energy also remain finite for finite d.

The experimental setup is usually defined as a (circular) capacitor partly filled with the liquid dielectric (He) (Refs. 1 and 5) and the electrons are localized at a dielectric surface by an image force and by an external electric field **E**. Therefore, instead of substracting the $\langle W_0^{ee} \rangle$ term from $\langle W^{ee} \rangle$, we now have to add the interaction of an electron with an external (pressing) field **E**. In the case of a constant field applied in the z direction, it becomes

$$\langle W^E \rangle = eE \langle z \rangle = eE \frac{3}{2\alpha} . \qquad (21)$$

When added to the electron energy, the term $\langle W^E \rangle$ can change, e.g., the optimized α values in the case of a free 2D electron gas.[14] However, in the case of a Wigner lattice, at typical electric fields $E \lesssim 500$ V/cm, the $\langle W^E \rangle$ term contributes much less to the total energy than the $\langle W^{ee} \rangle$ term for all relevant electron concentrations $(n > 10^8$ cm$^{-2})$.[1] It makes the optimized α values almost independent of E. Besides, all physical quantities, such as energy levels, that are measured with a finite electric field can be nicely extrapolated to the $E = 0$ limit.[1,14] In that sense all our results will be given for $E = 0$.

B. Optimized electron wave functions

In order to analyze the dynamical properties of a Wigner lattice on a dielectric with a metallic substrate, we first have to determine the variational parameter α, by minimizing the Hartree Hamiltonian of the whole system[7] for a particular electron density and thickness of the dielectric layer. In all calculations we assume a 2D hex-

agonal Wigner lattice with the lattice parameter r_0 and the average surface per electron $S = \sqrt{3}/2r_0^2$.

Following the procedure described in I, with the function $f(x)$ defined in the Appendix and with the $\langle W_0^{ee} \rangle$ term included, we obtain the parameter α for He ($\beta = 0.0278$) and Ar ($\beta = 0.248$) for three different thicknesses d of a dielectric layer (Fig. 1).

The α values start to deviate from the $d \to \infty$ limit for rather thin films $d \lesssim 100$ Å, a consequence of the screening effect. For thinner dielectric layers, the influence of the metallic substrate and therefore the influence of image potential on the total electron energy obviously becomes more important, which increases the localization of the electron wave function (10). However, at the same time [see Eqs. (14) and (15)], the screened electron-electron interaction becomes less repulsive, which in turn weakens the lattice potential. In the high-density region, the second effect overcomes the first, so in that region the electrons on a thin dielectric layer become more delocalized as compared to the $d \to \infty$ limit.

C. Dispersion relations

Determination of the parameter $\alpha(r_0, d)$ enables us to discuss the dynamical properties of electronic Wigner lattices (II, Appendix A). Figure 2 shows the vibrational modes $\omega_\pm(\mathbf{k})$ of a Wigner lattice on He and Ar layers as compared to the classical results ($\alpha \to \infty$, $\epsilon \to 1$).[3] The classical curve is *between* the He and Ar curves. It means that the classical electrons are screened more efficiently than the "delocalized" electrons on the He substrate, but still less than the electrons on the Ar substrate. As pointed out earlier, the presence of a metallic substrate leads to the complicated localization-delocalization effect, which depends on both the electron density and the dielectric layer thickness, and one cannot expect a simple behavior, like the "frequency lowering in the He-Ar order," as in the classical $d \to \infty$ case.[8]

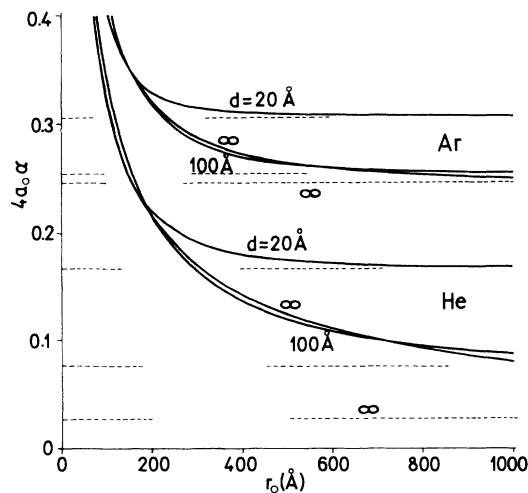FIG. 1. Optimized values of α (in units $4a_0$) for He and Ar layers as functions of the lattice parameter r_0. The straight dashed lines represent the asymptotic ($r_0 \to \infty$) values.

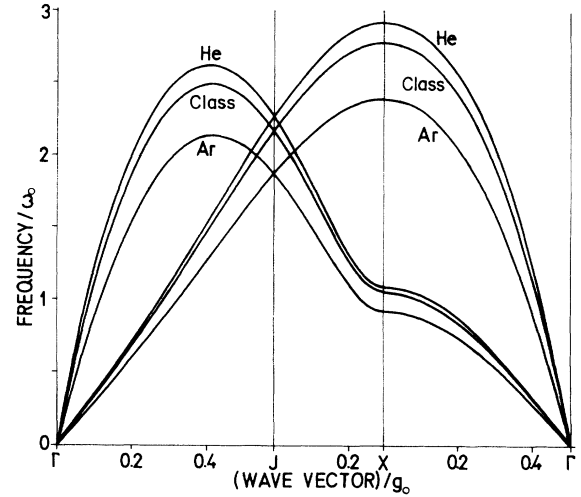FIG. 2. The frequencies of the two phonon modes for the 2D hexagonal electron lattice. We take $r_0 = 300$ Å and $d = 100$ Å. The frequencies are shown in units $\omega_0 = (e^2/m\, r_0^3)^{1/2}$ and the wave vectors in units of the reciprocal-lattice vector $g_0 = 4\pi/\sqrt{3}r_0$.

D. Ground-state energy

The total ground-state energy of the Wigner lattice (per one electron),[8,10]

$$E_g = \sum_p \frac{\hbar}{2} \langle \omega_p \rangle + \langle E^{im} \rangle + \tfrac{1}{2} \langle W^{ee} \rangle , \tag{22}$$

contains two "static" contributions $\langle E^{im} \rangle$ and $\langle W^{ee} \rangle$, which we have already discussed, and the dynamical contribution from the two phonon modes $p = (+, -)$. Here $\langle \omega_p \rangle$ is the frequency of the p mode averaged over the first Brillouin zone and this contribution to E_g is calculated following II and the Appendix.

When calculating the ground-state energy, we shall still first substract the $\langle W_0^{ee} \rangle$ term from it, for two reasons:

(i) The numerical calculation of $\langle W^{ee} \rangle - \langle W_0^{ee} \rangle$ is much easier than the $\langle W^{ee} \rangle$ term alone, as shown in the Appendix.

(ii) The $\langle W_0^{ee} \rangle$ term can than be added in the explicit form (20). Moreover, this form enables us to add only the second part of (20), which contains the parameter α:

$$\langle W_{00}^{ee} \rangle = \frac{2\pi}{S} e^2 \frac{33}{16} \frac{1}{\alpha} . \tag{23a}$$

The first term in (20)

$$\langle W_{0d}^{ee} \rangle = \frac{2\pi}{S} e^2 \left| \frac{1-\beta}{1+\beta} \right| 2d , \tag{23b}$$

remains fixed for a given system, so we can take it as a level from which we shall measure E_g. Defined as such, the ground-state energy remains finite even at the $d \to \infty$ limit. In the point-electron approximation ($\alpha \to \infty$), the term $\langle W_{00}^{ee} \rangle$ is zero, so the usual substraction of the $\langle W_0^{ee} \rangle$ term from the total electron energy[2,3] means that the energy is measured from the same level as in our case.

This will enable us to compare the results.

Figure 3(a) shows E_g for three different thicknesses d of He and Ar layers. At low densities E_g is mainly determined by the image potential and therefore depends strongly upon the dielectric thickness d. However, at high densities ($r_0 \lesssim 100$ Å) the influence of the lattice potential increases and E_g becomes almost independent of d. The classical values for E_g are close to the He and Ar values at low densities and differ drastically from them at high densities, as the classical curve for $d = 100$ Å illustrates. This difference is mainly due to the $\langle W_{00}^{ee} \rangle$ term, whose repulsive influence becomes important at $r_0 < 400$ Å.

The $\langle W_{0d}^{ee} \rangle$ term depends upon r_0, so we have to include it to obtain the true dependence $E_g(r_0)$, as shown in Fig. 3(b). However, here we divide E_g by d in order to obtain all curves on the same scale. In that sense, the

$d \to \infty$ limit means the case $d \gg r_0$, i.e., only the $\langle W_{0d}^{ee} \rangle$ term remains.

The extremely large increase of E_g in the region of small lattice parameters ($r_0 < 200$ Å) shows that one cannot easily stabilize the Wigner lattice at electron concentrations greater than $n_{max} \approx 3 \times 10^{11}$ cm^{-2}, regardless of the dielectric layer thickness, so we tentatively interpret n_{max} as a maximum electron concentration to which the smooth dielectric surface can be charged. It agrees with the present experimental situation in the sense that n_{max} represents an upper limit, because we have not taken into account other effects (surface roughness, tunnel effect, etc.) that can also destabilize a charged surface.[6] The large increase in E_g is mainly caused by the $\langle W_0^{ee} \rangle$ term, which explains why this effect was not obtained in the $d = \infty$ case[7,8] or in the classical limit.[3]
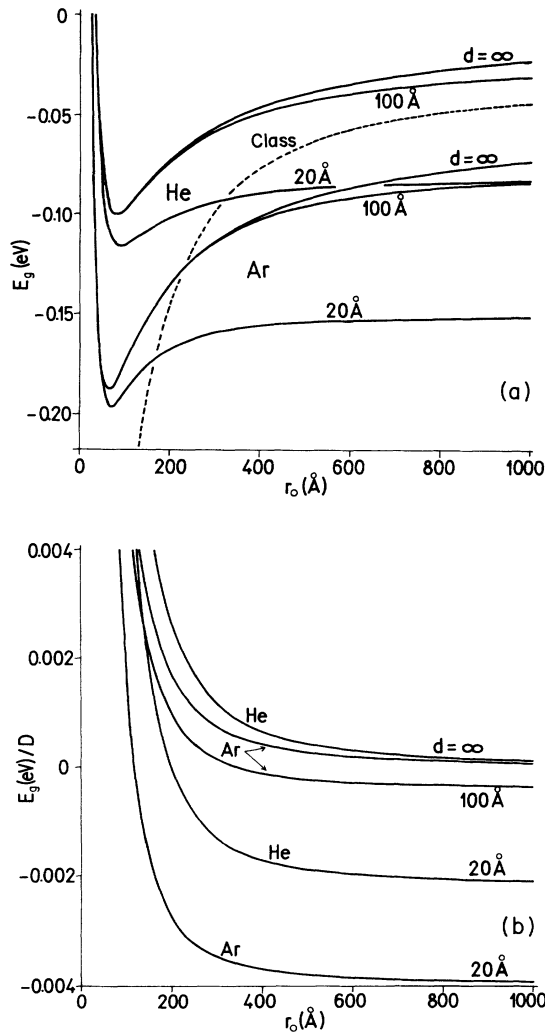

FIG. 3. The ground-state energy per one electron, for 2D hexagonal lattices on He and Ar layers, as a function of the lattice parameter r_0. (a) Without the $\langle W_{0d}^{ee} \rangle$ term. The dashed line represents the classical point-electron values. (b) With the $\langle W_{0d}^{ee} \rangle$ term, and divided by $D = d/a_0$. The $d = 100$ Å He curve (not shown) lies slightly below the $d = \infty$ He curve.
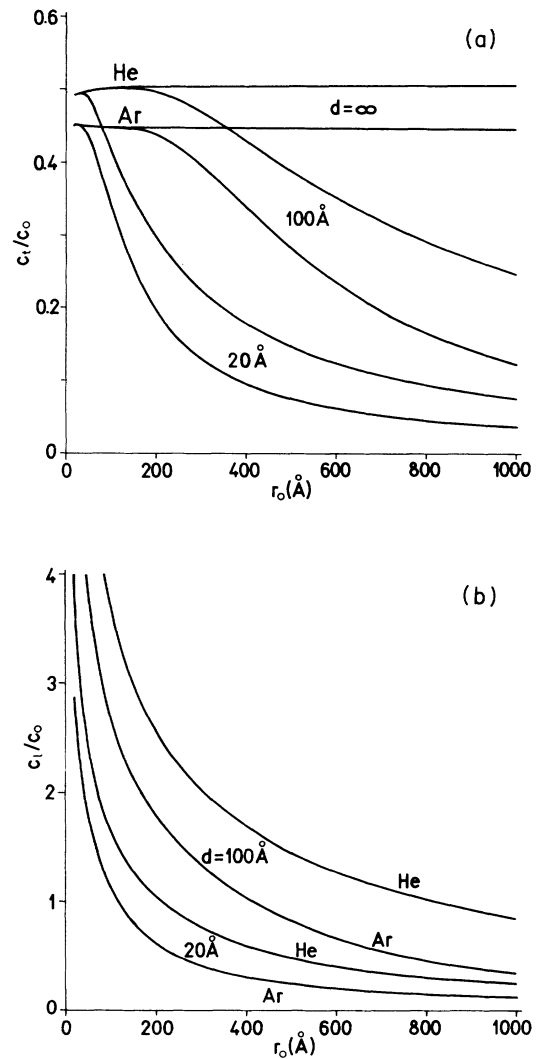

FIG. 4. The transverse (a) and longitudinal (b) sound velocities, for the 2D hexagonal lattices on He and Ar layers, as functions of the lattice parameter r_0, in units $c_0 = \omega_0 r_0 = (e^2/m\, r_0)^{1/2}$.

E. Sound velocities

Of particular interest is the behavior of the sound velocities of the Wigner lattice, defined as

$$c_t = \lim_{k \to 0} \left| \frac{\partial \omega_-}{\partial k} \right|, \quad c_l = \lim_{k \to 0} \left| \frac{\partial \omega_+}{\partial k} \right|. \quad (24)$$

Figures 4(a) and 4(b) show strong dependence of the transverse c_t and longitudinal c_l sound velocities on the lattice parameter r_0 for finite thicknesses of a dielectric layer. Notice that c_l becomes infinite in both the $d \to \infty$ and $r_0 \to 0$ limits. In these two cases, the lattice behaves as a 2D Coulomb system, with $\omega_+ \sim k^{1/2}$ in the long-wavelength $(k \to 0)$ limit. In particular, for $d \to \infty$, $c_t \sim 1/r_0^{1/2}$ in the $r_0 \to \infty$ limit, so c_t/c_0 remains finite.[8,3] However, for finite d, in the $r_0 \to \infty$ (i.e., $r_0 \gg d$) limit, $(c_t, c_l) \sim 1/r_0^{3/2}$, so both c_t/c_0 and c_l/c_0 tend to zero as $1/r_0$. Let us also mention that the classical values (not shown) again fall between the He and Ar values.

IV. THE WIGNER PHASE TRANSITION

The existence of a (2D) Wigner lattice was experimentally first confirmed by Grimes and Adams,[1] who detected the phase transition. Following the same procedure as in II, we use the theories of Kosterlitz and Thouless[15] and Halperin and Nelson[16] and Young[17] (KTHNY) define the melting temperature T_m:

$$\frac{k_B T_m}{V_0} = \frac{F}{\Gamma_0} . \quad (25)$$

Here V_0 is the bare Coulomb potential, and for the parameter Γ_0 we take the renormalized value $\Gamma_0 = 137$.[18] The d dependence enters only through the function F:[8]

$$F = (1 - c_t^2/c_l^2) c_t^2/c_{t0}^2 , \quad (26)$$

where $c_{t0} = 0.513 c_0$ is the transverse sound velocity in the classical limit.

Figures 5(a) and 5(b) show the phase diagrams of the Wigner lattice on He and Ar layers of different thicknesses, respectively. The line that defines the Fermi temperature T_F for a given electron concentration n divides the classical $(T > T_F)$ from the quantum $(T < T_F)$ region. The parameters n_0 and T_0,[8,3] defined by

$$n_0 = \frac{4}{\pi} \frac{1}{(a_0 \Gamma_0)^2}, \quad k_B T_0 = \left[\frac{e^2}{a_0} \right] \frac{2}{\Gamma_0^2} \quad (27)$$

take the values $n_0 = 2.42 \times 10^{12}$ cm^2, $T_0 = 33.6$ K for $\Gamma_0 = 137$.

Notice that the kinetic energy E_k of a "free 2D electron" can be approximated by $E_k(T) \approx k_B T$ in the classical regime and by $E_k(T) \approx \frac{1}{2} k_B T_F$ in the quantum regime. Therefore, if one tries to generalize the melting criterion (25) by substituting[3]

$$k_B T_m \to E_k(T_m) , \quad (28)$$

the effect will be evident mainly in the quantum regime. The influence of the dielectric constant on the phase diagrams without the metallic substrate was extensively discussed in Ref. 8, and here we shall be particularly interested in their thickness dependence for *low densities and temperatures*.

(i) For *thick dielectric layers* $(d > 100$ Å$)$ the melting curves at low n and T lie in the classical regime. In fact, at higher temperature $(T \geq 0.3 T_0)$ they approach the $T = T_F$ line, and in that case the replacement (28) leads to the bending of the curves upwards, but they reach the $T = 0$ line[8,3] at very high electron concentrations $(n \sim n_0)$, which are outside the experimental possibilities and our considerations. (ii) In the case of *thin dielectric layers* $(d < 100$ Å$)$ the whole melting curve can lie in the quantum regime, and now the choice of the expression for the kinetic energy becomes crucial.

Figure 5 clearly shows the decrease of the crystalline region for a lower dielectric thickness and higher dielectric constant. The reason for such behavior is a strong image force acting on electrons above a thin dielectric layer with a metallic substrate, or above a layer with a
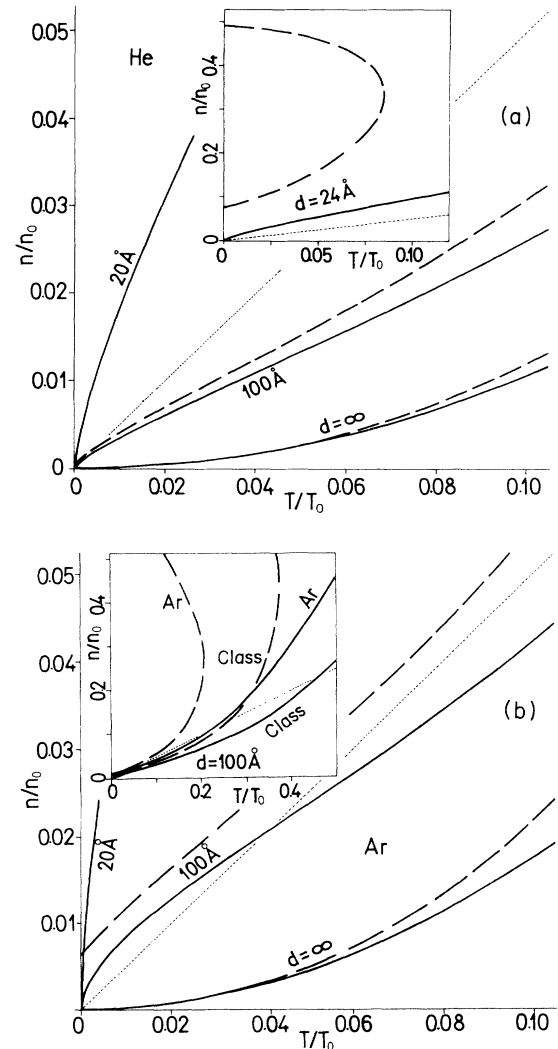

FIG. 5. Phase diagrams for the Wigner crystallization on (a) He and (b) Ar layers. The straight dotted line represents the $T_F(n)$ curve, and the dashed lines are obtained with the replacement (28).

relatively high dielectric constant. As shown in Sec. II, it leads to a weak (dipolar) electron-electron interaction at low electron concentrations, where the lattice becomes unstable. However, the melting curves obtained from the standard melting criterion (25) always start from the $(T=0, n=0)$ point and therefore predict the existence of the Wigner lattice at low electron concentrations for all thicknesses of a dielectric layer. On the other hand, with the replacement (28), the kinetic energy in the quantum regime becomes finite at the $T\rightarrow 0$ limit, so it can dominate over the weak potential energy, which further reduces the crystalline phase. As a consequence, a Wigner lattice cannot exist on a dielectric layer that is thinner than some critical thickness d_c. We find $d_c=22$ Å for He and $d_c=39$ Å for Ar. For each $d>d_c$ we can then determine a critical density $n_c(d)$ below which a Wigner lattice is not possible even at $T=0$. This is demonstrated in the inset of Fig. 5(a), where we put $d=24$ Å, i.e., slightly above d_c for He, and obtain $n_c\approx 0.07n_0\approx 1.7\times 10^{11}$ cm^{-2}. Notice that with increasing d, the critical density n_c decreases and we find $n_c\rightarrow 0$ for $d\rightarrow \infty$.

A similar discussion was performed in Refs. 2 and 3 within the classical model. Again, the melting curves obtained from this model fall between the corresponding He and Ar curves. Particularly, with the replacement (28), the Wigner crystal cannot exist below $d_c=31$ Å in the classical model, while it exists in our model on the He substrate. This is due to large delocalization of electrons in the Wigner lattice. On the other hand, the fact that d_c is higher in the case of the Ar substrate than in the classical model is caused mainly by the influence of the Ar dielectric constant ($\epsilon=1.66$), which cannot be ignored as in the classical case ($\epsilon=1$). The difference between the Ar and classical melting curves is illustrated in the inset of Fig. 5(b) for $d=100$ Å.

Bearing in mind that thin dielectric layers on a metallic substrate can support higher electron concentrations, we expect that experiments in this configuration could provide answers to the questions of whether the KTHNY theory is correct, whether the replacement (28) is valid, and whether the influence of the substrate dielectric constant and the electron delocalization is properly described in our model.

Finally, we want to comment on the agreement between the experiment and the theory we have derived in Ref. 19, where we have used the replacement (28) and taken into account only the influence of the image potential in the calculation of α. In this specific experiment,[5] the dielectric thickness was $d\gtrsim 240$ Å, and we see from the present calculation that the replacement (28) had no influence on T_m. Also, the lattice parameter was $r_0\gtrsim 940$ Å and the influence of the image potential was dominant. Therefore, the present theory, which improves upon the calculation,[19] would also be in very good agreement with these experimental data.

V. CONCLUSION

We have analyzed the influence of a metallic substrate placed below a dielectric film on the electronic Wigner lattice above this film. We evaluated results for three representative thicknesses of a dielectric film: $d=20$ Å as an extremely thin dielectric film, in order to clarify the influence of a metallic substrate; $d\rightarrow \infty$ as a limiting case, in which the dielectric plays a dominant role; and $d=100$ Å as an intermediate case, in which the dielectric properties of the layer and the influence of the metallic substrate are of comparable importance.

The influence of electron delocalization on the properties of the Wigner lattice was discussed earlier in the $d=\infty$ case.[7,8] Here we have shown that this influence becomes particularly important for thin dielectric layers on a metallic substrate, where delocalized electrons feel much lower image force than the point electrons on a dielectric surface. The influence of the dielectric substrate was analyzed by calculating and comparing all the Wigner lattice properties for He and Ar. Notice that both of them produce a strong repulsive potential at the surface due to the excitation gap in the rare-gas layer. As a consequence of complicated effects of electron delocalization and the thin-film dielectric constant on the Wigner lattice, the results obtained in the classical model ($\Delta z\rightarrow 0$, $\epsilon\rightarrow 1$) usually lie between the results for He and Ar.

Particular attention was paid to the boundary conditions satisfied by the 2D electron lattice in a realistic experimental situation. It was shown that the $k=0$ component of the lattice potential should be taken into account even in the $d\rightarrow \infty$ limit, in order to obtain correct behavior of the system at higher electron densities. This term was omitted in the $d=\infty$ (no metallic substrate) case,[7,8] where different boundary conditions should be applied in order to make the whole system neutral. We have outlined how different results arise in these two physical situations.

We also derived melting curves of a Wigner lattice using the KTHNY theory and its "extension" into the quantum regime. Without trying to give a definite answer, we suggest some critical experiments that could provide more information about this intriguing system.

Finally, we point out that in this paper we continued the systematical approach to the Wigner lattice, developed in I and II for the semi-infinite dielectric substrate, and, within the same formalism, were able to derive the properties of the Wigner lattice on a thin dielectric layer placed above a metallic substrate.

ACKNOWLEDGMENT

APPENDIX: LATTICE SUMMATION AND DEFINITION OF THE FUNCTION $f(x)$

In Sec. II we discussed the influence of the metallic substrate placed below the finite dielectric layer on the electron-electron interaction $\langle W^{ee}(\rho)\rangle$. We pointed out that this influence is taken into account if one simply changes $\beta\rightarrow D(k)$ in $W^{ee}(k;z,z')$, given by Eq. (6) of Ref. 7. Following the Appendix I and using the expansion (5) for $D(k)$, we can again perform the transformation [Eq. (A6), Ref. 7] from the "k space" to the "x space." It

gives the interaction between two electrons at their lateral sites (ρ_0, ρ_l) in the form

$$\langle W^{ee}(\rho_{0l}) \rangle = e^2 \frac{2}{\sqrt{\pi}} \int_0^\infty dx \, e^{-(\rho_0 - \rho_l)^2 x^2} f(x) , \tag{A1}$$

appropriate for the Ewald transformation and the lattice summation. The function $f(x)$ [Eq. (A7), Ref. 7] is now defined as

$$f(x) = \int dz \int dz' |u(z)|^2 |u(z')|^2$$

$$\times \left[e^{-(z-z')^2} - \sum_{n=-1}^\infty b_n e^{-[z+z'+2(n+1)d]^2 x^2} \right] . \tag{A2}$$

Inserting $u(z)$, Eq. (10), in (A2) we obtain

$$f(x) = f^e(x) + f^i(x) , \tag{A3}$$

where the first term $f^e(x)$ is the direct electron-electron interaction

$$f^e(x) = \tfrac{1}{8} \int_0^\infty dy (y^2 + 3y + 3) e^{-y} e^{-(x/2\alpha)^2 y^2} , \tag{A4}$$

while the second term $f^i(x)$ represents the interaction of

one electron with all images of the other electron:

$$f^i(x) = \sum_{n=-1}^\infty b_n f_n^i(x) , \tag{A5a}$$

$$f_n^i(x) = \tfrac{1}{120} \int_0^\infty dy \, y^5 e^{-y} e^{-(x/2\alpha)^2 [y+4\alpha(n+1)d]^2} . \tag{A5b}$$

For small β ($\beta \lesssim 0.3$), following Eq. (8), one has to take into account only the first three terms in (A5a).

In the limit $d = \infty$ only the $n = -1$ term remains, with $b_{-1} = \beta$, in agreement with the expression (A7), (Ref. 7) for $f(x)$. The integration in (A4) and (A5) can be performed analytically in the point-electron ($\alpha \to \infty$) approximation:

$$f(x) \xrightarrow[\alpha \to \infty]{} 1 - \sum_{n=-1}^\infty b_n e^{-[2d(n+1)]^2 x^2} . \tag{A6}$$

With the function $f(x)$ defined by Eqs. (A3)–(A5) we can continue the same procedure as in the Appendix of I, to obtain the lattice potential $\langle W^{ee} \rangle$ [Eq. (A13), Ref. 7] in the Hartree model.

One aspect of the influence of the metallic substrate on $\langle W^{ee} \rangle$ can be understood by analyzing the $x \to 0$ limit:

$$f(x \to 0) \to \begin{cases} \left[\dfrac{x}{2\alpha} \right]^2 \left[6 + \left[\dfrac{1-\beta}{1+\beta} \right] 4\alpha d \right]^2 , & x/\alpha \ll 1, \quad d \ll (1/x, 1/\alpha) \\ (1-\beta) + 6(7\beta - 1)(x/2\alpha)^2, & x/\alpha \ll 1, \quad d > 1/x . \end{cases} \tag{A7}$$

For $\beta = 1$ (i.e., $\epsilon = -\infty$) the dielectric layer becomes the same as the substrate (i.e., an ideal metal), so the thickness d has no influence on $f(x)$, and particularly $f(x \to 0) \to 36(x/2\alpha)^2$. For $\beta < 1$, $f(x \to 0)$ depends strongly on the dielectric thickness d. If we put $d = \infty$ before taking the $x \to 0$ limit, $f(x \to 0) = (1-\beta)$ remains finite. In that case, the lattice potential $\langle W^{ee} \rangle$, which contains the term [Eq. (A18), Ref. 7]

$$\frac{e^2}{S} 2\sqrt{\pi} \int_0^\eta dx \frac{f(x)}{x^2} , \tag{A8}$$

becomes infinite. It remains finite only in the presence of the metallic substrate, in which case $f(x \to 0) \sim x^2$. This statement is obviously equivalent to the charge-neutrality requirement (6), here transformed into "x space."

If we transform $\langle W_0^{ee} \rangle$ (18) in the "x space"

$$\langle W_0^{ee} \rangle = \frac{e^2}{S} 2\sqrt{\pi} \int_0^\infty dx \frac{f(x)}{x^2} , \tag{A9}$$

and substract it from the $\langle W^{ee} \rangle$ term, instead of (A8) the lattice sum will contain the term

$$\frac{e^2}{S} 2\sqrt{\pi} \int_\eta^\infty dx \frac{f(x)}{x^2} . \tag{A10}$$

This term is a smooth function of α, β, and d, and it remains finite in the $d \to \infty$ limit.

In Appendix A of II we have calculated the vibrational frequencies of the Wigner lattice using the dynamical matrix approach. The dynamical matrix (A2) (Ref. 8) is obtained by taking the derivatives of $\langle W^{ee}(\rho_{0l}) \rangle$ along the electron lateral coordinates, which leaves the function $f(x)$ unchanged. Therefore, the theory developed in Appendix A, paper II, can be applied in the case of a finite dielectric layer on a metallic substrate, provided that one takes the function $f(x)$ as defined by Eqs. (A2)–(A5) instead of its $d \to \infty$ limit (A7) (Ref. 7) or (A3b) (Ref. 8).

[1] C. C. Grimes and G. Adams, Phys. Rev. Lett. 42, 795 (1979).

[2] F. M. Peeters and P. M. Platzman, Phys. Rev. Lett. 50, 2021 (1983).

[3] F. M. Peeters, Phys. Rev. B 40, 159 (1984).

[4] M. Saitoh, Phys. Rev. B 40, 810 (1989).

[5] H. W. Jiang, M. A. Stan, and A. J. Dahm, Surf. Sci. 196, 1 (1988).

[6] X. L. Hu and A. J. Dahm, Phys. Rev. B 42, 2010 (1990).

[7] Z. Lenac and M. Šunjić, Phys. Rev. B 43, 6049 (1991).

[8] Z. Lenac and M. Šunjić, Phys. Rev. B 44, 11 465 (1991).

[9] M. W. Cole, Phys. Rev. B 3, 4418 (1971).

[10] L. Bonsal and A. A. Maradudin, Phys. Rev. B 15, 1959 (1977).

[11] G. Meissner, H. Namaizawa, and M. Voss, Phys. Rev. B 13, 1370 (1976).

[12] M. Saitoh, J. Phys. Soc. Jpn. 42, 201 (1977).

[13] B. Trninić-Radja, M. Šunjić, and Z. Lenac, Phys. Rev. B 40, 9600 (1989).

[14] C. C. Grimes, T. R. Brown, M. L. Burns, and C. L. Zipfel, Phys. Rev. B 13, 140 (1976).

[15] J. M. Kosterlitz and D. J. Thouless, J. Phys. C 6, 1181 (1973).

[16] D. R. Nelson and B. I. Halperin, Phys. Rev. B 19, 2457 (1979).

[17] P. Young, Phys. Rev. B 19, 1855 (1979).

[18] M. A. Stan and A. J. Dahm, Phys. Rev. B 40, 8995 (1989).

[19] M. Šunjić and Z. Lenac, Europhys. Lett. 11, 431 (1990).